26. Round, E. F., Crawford, R. M. and Mann, D. G., In *The Diatom Biology and Morphology of Genera*, Cambridge University Press, Cambridge, 1990, pp. 7–20.
27. Traverse, A., *Sedimentation of Organic Particles*, Cambridge University Press, New York, 2005, p. 544.
28. Roncaglia, L., Palynofacies analysis and organic walled dinoflagellate cysts as indicators of paleo-hydrographic changes: an example from Holocene sediments in Skalafjord, Faroe Islands. *Mar. Micropalaeontol.*, 2004, **50**, 21–42.
29. Prasad, V., Garg, R., Singh, V. and Thakur, B., Organic matter distribution in Arabian Sea: Palynofacies analysis from the surface sediments off Karawar coast (west coast of India). *Indian J. Mar. Sci.*, 2007, **36**, 399–406.
30. Haseldonckx, P., A palynological interpretation of palaeoenvironment in S.E. Asia. *Sains Malays.*, 1974, **3**, 119–127.
31. Hart, G. F., Origin and classification of organic matter in the clastic systems. *Palynology*, 1986, **6**, 1–7.
32. Pocock, S. A. J., Vasanthy, G. and Venkatachala, B. S., Introduction to the study of particulate organic materials. *J. Palynol.*, 1987, **23**–**24**, 167–188.
33. Tyson, R. V., *Sedimentary Organic Matter: Organic Facies and Palynofacies*, Chapman & Hall, London, 1995, p. 615.
34. Batten, D. J., Palynofacies, paleoenvironment and petroleum. *J. Micropaleontol.*, 1982, **1**, 107–114.
35. Battarbee, R. W., Diatom analysis. In *Handbook of Holocene Palaeoecology and Palaeohydrology* (ed. Berglund, B. E.), Wiley, 1986, pp. 527–570.
36. vonWaveron, I. V. and Visscher, H., Analysis of the composition and selective preservation of organic matter in surficial deep sea sediments from a high productivity area (Banda Sea, Indonesia). *Palaeogeogr., Palaeoclimatol., Palaeoecol.*, 1994, **112**, 85–111.
37. Tyson, R. V. and Follows, B., Palynofacies prediction of distance from sediment source: a case study from the Upper Cretaceous of the Pyrenees. *Geology*, 2000, **28**, 569–571.
38. Roncaglia, L., Revision of the palynofacies model of Tyson (1993) based on recent high-latitude sediments from the North Atlantic. *Facies*, 2006, **52**, 19–39.
39. Zonneveld, K. A. F. and Jurkschat, T., *Bitectatodinium spongium* (Zonneveld, 1997) Zonneveld et Jurkschat, comb. nov. from modern sediments and sediment trap samples of the Arabian Sea (northwestern Indian Ocean): taxonomy and ecological affinity. *Rev. Palaeobot. Palynol.*, 1999, **106**, 153–169.
40. Prakash, S. and Ramesh, R., Is the Arabian Sea getting more productive? *Curr. Sci.*, 2007, **92**, 667–671.
41. George, M. J., Studies on the prawn fishery of Cochin and Alleppey coasts. *Indian J. Fish.*, 1961, **8**, 75–95.
42. Harold, G., Marshall, R. and Alden, W., A comparison of phytoplankton assemblages and environmental relationships in three estuarine rivers of Lower Chesapeake Bay. *Estuaries*, 1990, **13**, 287–300.
43. Cooper, S. R., Estuarine paleoenvironmental reconstructions using diatoms. In *The Diatoms: Applications to the Environmental and Earth Sciences* (eds Stoermer, E. F. and Smol, J. P.), Cambridge University Press, Cambridge, 1999, pp. 352–373.

ACKNOWLEDGEMENTS. We thank the Director, BSIP, Lucknow for providing facilities to carry out this work. We also thank Dr Madhav Kumar, BSIP, Lucknow for providing the samples for the present study and Mr Kusum Karati, NIO, Kochi for valuable suggestions.

Received 3 November 2011; revised accepted 21 August 2012

Occurrence of rhyolite in Jangalgali Formation, Jammu and Kashmir, Northwest Himalaya, India

N. Siva Siddaiah* and M. K. Shukla

Wadia Institute of Himalayan Geology,
33, General Mahadeo Singh Road, Dehra Dun 248 001, India

We report here the occurrence of rhyolite between the Neoproterozoic Sirban Limestone and Palaeogene Subathu Formation in Northwest Himalaya, India. It is 5–10 m thick, consists of phenocrysts of quartz and feldspars of different shapes and sizes distributed randomly in a glassy matrix. Zircon, rutile, biotite, tourmaline and haematite occur in minor amounts. Bipyramidal, angular and skeletal morphologies are common in quartz. Quartz shows resorption features and contains inclusions of negative crystals. The field feature, mineralogy, texture and whole-rock composition are typical of high-silica rhyolites. By virtue of its occurrence at the base of the Himalayan foreland stratigraphy, the rhyolite is important in exploring the timing of India–Eurasia primordial collision and in stratigraphic correlation studies.

Keywords: Himalayan foreland basin, Palaeogene Subathu Formation, rhyolite.

THIS study reports the occurrence of rhyolite between the Neoproterozoic Sirban Limestone and Early Palaeogene Subathu Formation in Jammu region, Jammu and Kashmir (J&K) Himalaya, India (Figure 1)[1]. The lithounits sandwiched between Sirban Limestone and Subathu Formation in J&K are known as Jangalgali Formation and/or Khairikot Formation consisting of bauxite/laterite, rhyolite in addition to chert and variegated shale[2,3]. Although several biostratigraphic studies have been carried out on syn-orogenic sediments of the Subathu Formation because of their abundant and well-preserved fauna and hydrocarbon potential[4–10], there are no systematic studies on the lithounits that make up the Jangalgali Formation. Characterizing and determining the origin and age of the rocks of the Jangalgali Formation is important for a variety of reasons, including understanding their relation, if any, to India–Eurasia initial collision. As part of this objective, we present here results of our studies on the geological occurrence, field features, mineralogy and textural characters of silicic units of the Jangalgali Formation which were described in the literature as 'chert breccia', demonstrate their rhyolitic nature and discuss their importance in the Himalayan orogeny.

Regional geology and stratigraphic relations among Sirban Limestone, Subathu Formation and Jangalgali

*For correspondence. (e-mail: nssiddaiah@rediffmail.com)

Formation have been studied by several researchers[2–5,8,10–14]. A brief account of the same is provided here.

The lithounits in the study area mainly belong to the Murree (late Eocene to early Miocene) and Subathu (late Palaeocene to middle Eocene) Groups, resting unconformably on the Jangalgali Formation. The sediments of the Murree Group are the youngest and occupy the largest area in the region. The unconformity between the Sirban Limestone and the Subathu Formation is marked mainly by rhyolite and bauxite of the Jangalgali Formation (Figure 2). The Jangalgali Formation is exposed in different localities of J&K. At Kalakot, Beragua and Khargala only rhyolite is exposed; at Muttal, Jangalgali and Reasi only bauxite is exposed, and at Salal both rhyolite and bauxite are present. On the basis of geochemical data, basalt to basaltic andesites have been suggested as protoliths for bauxite deposits[15]. Based on the presence of index foraminifera like *Daviesina garumnensis*, *Ranikothalia nuttalli* and *Lockhartia*, a late Thanetinian age (56 Ma) is assigned for the basal part of the Subathu Formation at Kalakot in Jammu region[9]. The exposures of Sirban Limestone are found mainly as inliers, occupying the crestal part of anticlinal features. Based on the presence of stromatolites, a Neoproterozoic age is suggested for the Sirban Limestone[14]. The outcrops of rhyolite exposed along road cuts and creeks were examined for physical properties as well as field relation with the associated lithounits. A total of 75 samples of rhyolite were collected for mineralogical, textural and geochemical studies.

Rhyolite by virtue of its high silica content forms a physically and chemically distinct unit relative to the rest of the lithounits in the studied area. Its distribution is widespread in and around villages of Kalakot, Beragua, Khargala and Tattapani in Rajauri District and Kanthan in Reasi District, J&K (Figure 1). The rhyolite occurs unconformably over the Sirban Limestone. It is overlain by a thin but inpersistent horizon of bauxite (Figure 2). Rhyolite is grey to brown, hard, with thickness varying from 5 to 10 m. Its contact with the Sirban Limestone is generally obscured, but the upper contact with Subathu shale is well exposed and sharp in all the localities studied. A brief description of the rhyolite exposed in different parts of Jammu region is presented in Table 1.

Rhyolite is porphyritic (~ 10–15 volume % phenocrysts). Phenocrysts of quartz and K-feldspar are set in a fine-grained glassy matrix and lack preferred orientation (Figure 3). Freshly exposed outcrop surfaces appear glassy. The rock breaks with conchoidal fracture.

Phenocrysts are of large angular and euhedral to subhedral quartz and plagioclase with subsidiary sanidine dispersed in a microcrystalline to glassy groundmass. Among the phenocrysts, quartz is the most abundant. Most of the larger crystals are sharp and fresh in appearance, but edges of the smaller grains are corroded or rounded. Accessory minerals such as zircon, rutile, haematite and tourmaline occur as small euhedral to subhedral crystals. The groundmass constitutes a major component of the rhyolite. Light yellowish-brown, 50–150 μm prismatic crystals of zircon (Figure 4 *a*), and large (often larger than 100 μm) brownish/reddish rutile occur as in the glassy matrix (Figure 4 *b*). Haematite is bright red, occurs as well-developed rhombohedral crystals and as embayed grain disseminations within the matrix. Its presence suggests oxygen-rich nature of the magma.

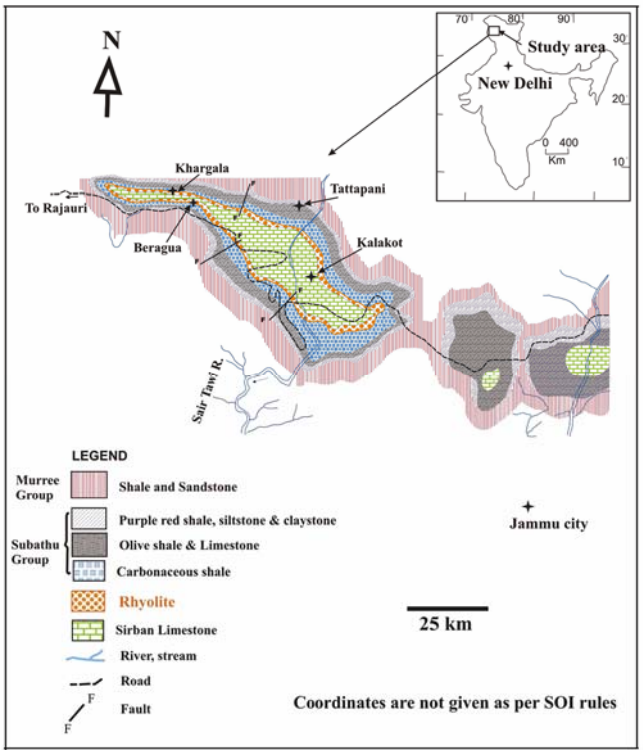

Figure 1. Generalized geological map of Jammu region showing the localities (except Kanthan) of rhyolite (modified after Rao and Rao[1]).

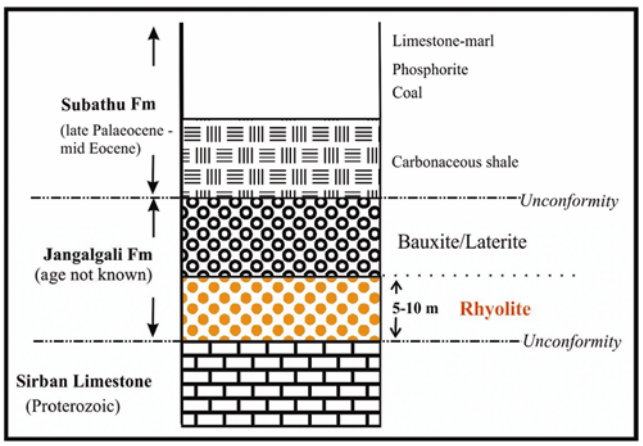

Figure 2. Simplified litholog of Jammu region showing the stratigraphic position of rhyolite in the unconformity zone of Jangalgali Formation.

Table 1. Field features of rhyolite at different localities in Jammu region

Locality	Field description
Kalakot (~ 120 km northwest of Jammu city)	Rhyolite is exposed on either side of the bridge on the stream (Sair Tawi) draining country on the west side of the village. It is ~ 5 m thick, lavender to grey, weathers tan to brown, and consists of phenocrysts ranging in size from a few millimetres to a couple of centimetres. GPS reading: 33°12′58″N, 74°24′58″E; elevation: 625 m.
Beragua and Khargala (~ 11 km west of Kalakot)	About 10 m thick rhyolite is exposed along the Kalakot–Rajauri road. It is porphyritic with ~ 10% phenocrysts of mainly quartz and sanidine enclosed in a glassy matrix. The size of phenocrysts ranges from a few millimetres to a couple of centimetres. GPS reading: 33°12′55″N, 74°24′04″E; elevation: 825.5 m for Beragua; and GPS reading: 33°14′10″N, 74°23′48″E; elevation: 900 m for Khargala.
Tattapani (~ 6 km west of Beragua)	Rhyolite is exposed along the right side of the road. It is ~ 5 m thick. The size of phenocrysts ranges from a few millimetres to a couple of centimetres. GPS reading: 33°14′25″N, 74°24′41″E; elevation: 798 m.
Kanthan (~ 20 km from Reasi town)	Rhyolite occurs ~ 1 km before Kanthan village on the left bank of the Chenab River, near the bridge. It is grey to pale red and ~ 10 m thick, prophyritic, with 10–15% phenocrysts of quartz, sanidine and minor plagioclase and biotite set in a glassy groundmass. GPS reading: 33°10′14″N, 74°51′04″E; elevation: 525.5 m.

Figure 3. Outcrop of rhyolite from Jangalgali Formation showing porphyritic texture (length of pen is ~ 15 cm).

Quartz in the studied rhyolite exhibits several distinct types of texture such as quartz-eye, partially resorbed/embayed, skeletal in addition to negative crystals and hexagonal bipyramidal forms. These striking textural features provide valuable information about how the rhyolitic melt crystallized. A brief description of these is as follows.

Quartz-eye: Two distinct types of quartz-eye are found in rhyolite. Type-1 consists of typical quartz phenocrysts (Figure 4 *c*) which are large (up to 8 mm in diameter), rounded and irregular. Individual crystals with distinct edges are dispersed throughout the groundmass. Type-2 quartz-eye is elliptical, small (< 2 mm) and consists of sugary aggregates of anhedral quartz crystals. These are different from type-1 and are interpreted as miarolitic pods. The quartz-eye represents quartz formed from an exsolved magmatic aqueous fluid during initial stages of its separation from a silicic magma[16,17]. Further, cooling during the course of crystallization of rhyolitic melts can lead to the generation of quartz-eye due to its ease of nucleation relative to other minerals[18].

Negative crystals: The melt inclusions observed in the quartz phenocrysts are randomly distributed in the host crystal. They vary from sub-rounded to negative crystal shapes with sizes ranging from < 5 to > 200 μm. Negative crystals often occur in clusters rather than individually and are commonly devitrified. The boundary between the negative crystal (melt inclusion) and the host quartz is sharp, and there is no trace of reaction between the two (Figure 4 *d*). Negative crystal inclusions are not present in all quartz phenocrysts; conversely, some quartz phenocrysts contain several inclusions of negative crystals. Based on their mode of occurrence, these inclusions are interpreted to be of primary origin. Similar observations have been reported by Lowenstern[19] and Clocchiatti[20] for naturally and experimentally heated volcanic rocks and by Frezzotti[21] for partly crystallized melt inclusions in granites. Skirius *et al.*[22] observed the transition of initially rounded melt inclusion into negative crystal shape during prolonged heating experiments. In addition, the observed negative crystals at the centre of quartz phenocrysts of the rhyolite from Jammu region may help constrain the primary chemical composition of the magma.

Bipyramidal quartz: Beta-quartz occurs as euhedral mostly hexagonal bipyramidal crystals (Figure 4 *e*). Some beta phases are highly spherical probably due to partial fusion in a liquid melt that was changing due to rapid

cooling during a volcanic eruption (Figure 4 *f*). Their presence as unstrained, single crystals up to 2 mm in size but without evidence of granulation indicates that they have a magmatic origin. This quartz morphology, especially the distinct bipyramids, is consistent with it being high-temperature beta-quartz commonly observed in volcanic rocks[23].

Embayed/resorbed quartz: Embayed and rounded quartz phenocrysts are common in the samples of this study. Re-entrants and in some cases embayments, along with irregular overgrowths, imply resorption. The general explanation is that rounded and embayed quartz is a product of decompression-induced stability field shift for quartz that occurs during magma ascent[24]. Some quartz grains develop highly angular and skeletal shape, and display jigsaw features which are attributed to *in situ* quench fragmentation (Figures 4 *g*). Embayed quartz has been interpreted to result from (i) adiabatic or sub-isothermal decompression making melt quartz undersaturated and leading to quartz resorption by the melt, and (ii) thermal disequilibrium by mixing with relatively high-temperature magma[25,26]. Nekvasil[27] showed that decrease in pressure can cause resorption of quartz, K-feldspar and plagioclase.

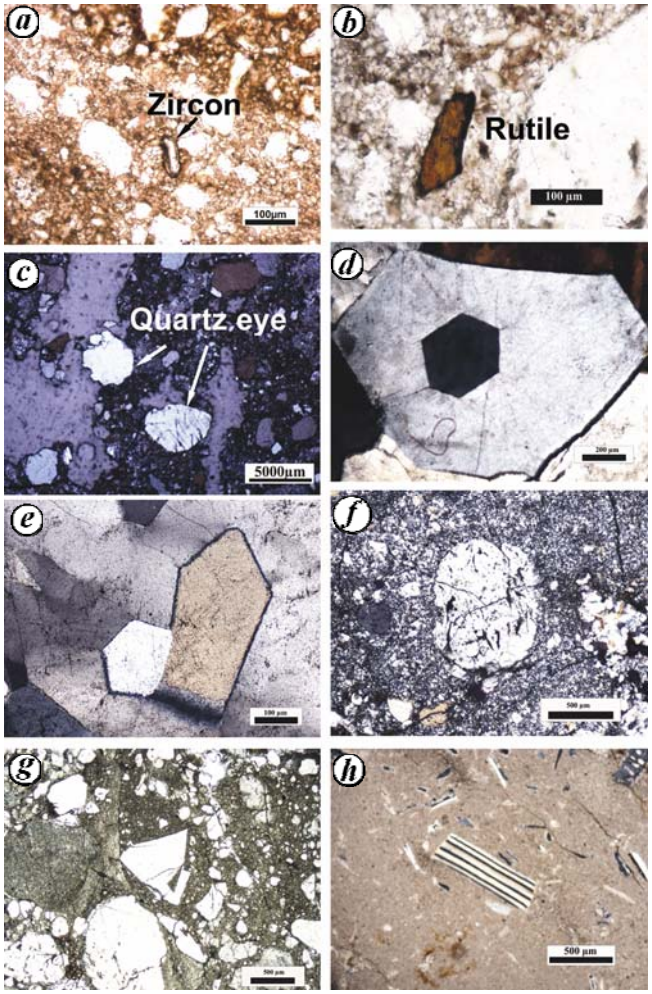

Figure 4. Photomicrographs of rhyolite from Jangalgali Formation. ***a***, Euhedral zircon (PPL). ***b***, Rutile (PPL). ***c***, Type 1 quartz eyes (CN). ***d***, Negative crystal having sharp contact with host quartz phenocryst (CN). ***e***, Hexagonal bipyramidal quartz crystals (CN). ***f***, Beta phase, spherical due to partial fusion in the melt (CN). ***g***, Quartz with skeletal texture (PPL). ***h***, Prismatic plagioclase with straight multiple albite twins (CN). PPL, Plane polarized light; CN, Crossed nicols.

Sanidine and plagioclase feldspar: Feldspars are the second most common phenocrystic phases after quartz in the studied rhyolite. They occur as euhedral to subhedral grains in brown, glassy groundmass. Sanidine occurs with euhedral to subhedral form and exhibits carlsbad twinning. Carlsbad twinning in the feldspar phenocrysts indicates that K-feldspar is primary. Plagioclase is present as prismatic crystals up to 700 µm in length and exhibits straight multiple albite twins (Figure 4 *h*).

The silicic rocks between the Neoproterozoic Sirban Limestone and Early Palaeogene Subathu Formation in Jammu region which have been described in the literature as chert breccias, display field, mineralogical and textural characteristics typical of a rhyolite described from elsewhere in the world[28–30]. The presence of hexagonal bipyramidal quartz, occurrence of quartz phenocrysts of different shapes and sizes with no preferred orientation, presence of high-temperature alkali-feldspar and grains with distinctive volcanic features like perfect crystal faces, inclusions with negative crystal shape, embayments, skeletal grains and rounded fractures all support volcanic origin for the rock.

The widespread occurrence of rhyolite with distinct textures and its stratigraphic position particularly at the base of the Early Palaeogene shallow marine sediments of the Himalayan foreland basin make it an important proxy for exploring its relation with India–Eurasia primordial collision and basin-wide stratigraphic correlation studies in a region that generally lacks similar useful marker units/horizons. Therefore, knowledge on the origin and absolute age of this rhyolite is warranted to understand better its significance in regional geology and India–Eurasia collision.

1. Rao, V. V. K. and Rao, R. P., Geology of the tertiary belts of Northwest Himalaya, Jammu and Kashmir State, India. *Geol. Surv. India, Misc. Publ*., 1979, **41**, 149–173.
2. Singh, P., The Subathu Group of India, Nav Jyoti Scientific Publications, Lucknow, Prof. Pap., 1980, vol. 1, p. 92.
3. Bhat, G. M. *et al.*, Biostratigraphy, structure and depositional environments of the Neoproterozoic Sirban Limestone, Proterozoic evaporite sequence and Tertiary succession of Jammu, India. In *Explanatory Notes and Field Excursion Guide*, Special Publication University of Jammu, 2008, vol. 2, pp. 1–75.
4. Singh, P., Larger foraminifera from Subathus of Bergua–Jangalgali area, J&K state. *J. Geol. Soc. India*, 1970, **11**, 34–44.
5. Singh, P. and Vimal, K. P., Discovery of stromatolites from the Sirban Limestone of Riasi, Jammu and Kashmir State. *J. Paleontol. Soc. India*, 1970, **15**, 6–9.

6. Acharyya, S. K. and Ray, K. K., Hydrocarbon potentiality of the Himalayan sedimentary infrastructure. *Geol. Surv. India, Misc. Publ*., 1979, **41**, 81–95.
7. Karunakaran, C. and Ranga Rao, A., Status of exploration for hydrocarbons in the Himalayan region – contribution to stratigraphy and structure. *Geol. Surv. India, Misc. Publ*., 1979, **41**, 1–67.
8. Nanda, A. C. and Kumar, K., *Excursion Guide on the Himalayan Foreland Basin* (*Jammu–Kalakot–Udhampur Sector*), Special Publication, Wadia Institute of Himalayan Geology, Dehradun, 1999, vol. 2, pp. 1–85.
9. Mathur, N. S. and Juyal, K. P., *Atlas of Early Palaeogene Invertebrate Fossils of the Himalayan Foothills Belt*, Monogr. Wadia Institute of Himalayan Geology, Dehradun, 2000, p. 257.
10. Singh, B. P., Evidence of growth fault and forebulge in the Late Palaeocene (57.9–54.7 Ma), western Himalayan foreland basin, India. *Earth Planet. Sci. Lett*., 2003, **216**, 717–724.
11. Medlicott, H. B., Notes on the Sub-Himalayan series in the Jammu (Jammoo) Hills. *Rec. Geol. Surv. India*, 1876, **9**, 49–57.
12. Wadia, D. N., The geology of Poonch State (Kashmir) and adjacent parts of Panjab. *Mem. Geol. Surv. India*, 1928, **51**, 257–268.
13. Middlemiss, C. S., Kalakot, Metka, Mahgola and other coalfields of Jammu Province. In Mineralogical Survey Report, Jammu and Kashmir Government, 1929, p. 116.
14. Raha, P. K. and Sastry, M. V. A., Stromatolites and Precambrian stratigraphy in India. *Precambrian Res*., 1982, **18**, 293–318.
15. Singh, B. P., Pawar, J. S. and Verma, M., Is Jammu bauxite a reworked basalt derived bauxite? *J. Geol. Soc. India*, 2005, **66**, 157–160.
16. Candela, P. A. and Blevin, P. L., Do some miarolitic granites preserve evidence of magmatic volatile phase permeability? *Econ. Geol*., 1995, **90**, 2310–2316.
17. Harris, A. C., Kamenetsky, V. S., White, N. C., van Achterbergh, E. and Ryan, C. G., Silicate-melt inclusions in quartz veins: linking magmas and porphyry Cu deposits. *Science*, 2003, **302**, 2109–2111.
18. Piccoli, P. M., Candela, P. A., Jugo, P. J. and Frank, M. R., Contrasting syn–late magmatic intrusive behavior of aplite dikes in the Tuolumne Intrusive Suite, California: implications for magma rheology. In Cordilleran Section of the Geological Society of America (a symposium in honor of Paul Bateman), 1996, vol. 28, p. 101.
19. Lowenstern, J. B., Dissolved volatile concentrations in an ore-forming magma. *Geology*, 1994, **22**, 893–896.
20. Clocchiatti, R., Les inclusions vitreuses des cristaux de quartz. Etude optique, thermooptique et chimique. Applications geologiques. *Mem. Soc. Geol. Fr.*, 1975, **122**, 1–96.
21. Frezzotti, M. L., Magmatic immiscibility and fluid phase evolution in the Mount Genis granite (southeastern Sardinia, Italy). *Geochim. Cosmochim. Acta*, 1992, **56**, 21–33.
22. Skirius, C. M., Peterson, J. W. and Anderson Jr, A. T., Homogenizing rhyolitic glass inclusions from the Bishop Tuff. *Am. Mineral*., 1990, **75**, 1381–1398.
23. Lowenstern, J. B. and Sinclair, W. D., Exsolved magmatic fluid and its role in the formation of comb-layered quartz at the Cretaceous Logtung W–Mo deposit, Yukon Territory, Canada. *Trans. R. Soc. Edinburgh Earth Sci*., 1996, **87**, 291–303.
24. McPhie, J., Doyle, M. and Allen, R., *Volcanic Textures. A Guide to the Interpretation of Textures in Volcanic Rocks*, Centre for Ore Deposit and Exploration Studies, University of Tasmania, Australia, 1993, p. 197.
25. Nakamura, M., Continuous mixing of crystal mush and replenished magma in the ongoing Unzen eruption. *Geology*, 1995, **23**, 807–810.
26. Sato, H., A model of the 1991 eruption of Unzen volcano inferred from petrographic textures of the ejecta. *Mem. Geol. Soc. Jpn*., 1996, **46**, 115–125.
27. Nekvasil, H., Ascent of felsic magmas and formation of rapakivi. *Am. Mineral*., 1991, **76**, 1279–1290.
28. Fink, J. H. and Manley, C. R., Origin of pumiceous and glassy textures in rhyolite flows and domes. *Geol. Soc. Am. Spec. Pap*., 1987, **212**, 77–88.
29. Manley, C. R. and Fink, J. H., Internal textures of rhyolites flows as revealed by research drilling. *Geology*, 1987, **15**, 549–552.
30. Siva Siddaiah, N., Origin of chert breccia at the unconformity between Precambrian Sirban Limestone and Paleogene Subathu Formation: evidence from Kalakot area, J&K Himalaya. *Curr. Sci.*, 2011, **100**, 1875–1880.

ACKNOWLEDGEMENTS. We thank the Director, Wadia Institute of Himalayan Geology, Dehra Dun for laboratory facilities. We also thank to Dr S. K. Pandita and Prof. G. M. Bhat, University of Jammu for help during field studies; Dr Kishor Kumar for useful suggestion and the anonymous reviewer for constructive comments.

Received 11 November 2011; revised accepted 16 August 2012

Rainfall interception in relation to the tree architecture of *Pinus wallichiana*

A.B. Jackson

M. A. Wani[1] and R. K. Manhas[1,2,*]

[1]Department of Botany, Government Sri Pratap College, Srinagar 190 001, India
[2]Present address: Department of Botany, Government Degree College, Kathua 184 104, India

Vegetation cover protects the topsoil by way of intercepting precipitation and reducing its direct impact on the soil. This communication presents the results of observations of rainfall interception in relation to the tree architecture and other features of *Pinus wallichiana* stand in Dal Lake catchment in Kashmir Himalayas. Stemflow (mm) was significantly ($P < 0.05$) influenced by diameter at breast height (DBH, cm), tree height (m), nature of bark and attachment angles of lateral branches in tree height resulted into 1.5% decrease in stemflow. Also, smooth-barked trees conducted around 5.0% more of stemflow than rough-barked ones. Throughfall decreased significantly ($P < 0.001$) with the increase in both DBH (cm) and height (m) and increased along the gradient of crown area. Throughfall was negatively correlated with downward branching pattern ($r = 0.83$; $P < 0.05$). Of the total average rainfall of 66.5 mm during the course of study, throughfall, stemflow and interception for the whole stand was calculated as 26.7%, 36.3% and 36.9% respectively. Interception percentage decreased significantly ($P < 0.001$) with increase in rainfall. The amount (mm) of interception ($r = 0.90$; $P < 0.001$), stemflow ($r = 0.96$; $P < 0.001$) and throughfall ($r =$

*For correspondence. (e-mail: manhasrk@rediffmail.com)